PRODUCTION OF NITROGEN OXIDE DURING CHAR OXIDATION AT PULVERIZED COAL COMBUSTION CONDITIONS

Alejandro Molina, Eric G. Eddings, David W. Pershing and Adel F. Sarofim
Department of Chemical and Fuels Engineering
University of Utah
Salt Lake City, UT 84112-1114

ABSTRACT

More stringent regulations for NO_x control in pulverized coal combustors have made the scientific community focus on sources of emissions that were traditionally considered less relevant to the overall NO_x production. The oxidation to NO of the nitrogen that is organically bound to the char is one of them. In this study, an experimental evaluation of the influence of the reduction of NO by char was carried out. The experiments with three different carbonaceous materials were conducted at temperatures close to that of pulverized combustion conditions (1700 K) in a laminar drop tube reactor and under inert and oxidizing atmospheres. The results obtained show that the process of NO reduction on the char plays an important role on the total amount of char-N converted to NO_x. This NO destruction pathway becomes less important at low NO background concentration and doesn't seem to strongly dependant on the char nature.

The predictions of a single particle model were compared to the experimental results. Although the model predicts a reduction on the conversion of char-N to NO that increases in proportion to NO concentration, it overpredicts the general value. A higher value for the rate of NO destruction on char surface doesn't seem to explain this phenomena that seems to be more related to the availability of char surface for the destruction of NO.

INTRODUCTION

Production of nitrogen oxide from fuel-nitrogen during coal combustion occurs by two different phenomena: *1.)* by the oxidation of the nitrogen released with the volatiles present in the char and *2.)* by the oxidation of the nitrogen that remains in the char matrix. Since the first mechanism occurs in the homogeneous phase, the production of NO_x through this path has traditionally been reduced by the same techniques that apply to the reduction of thermal NO. However, the heterogeneous nature of the second route had made it more difficult to develop effective procedures for its reduction. In addition, more stringent regulations for NO_x emissions increase the importance of the NO produced from char compared to that produced by the homogeneous route.

In order to attain a better understanding of the process of NO production during char oxidation, several single particle models have been proposed in the literature. Models for char-N evolution at fluidized bed combustor conditions [1-3] are concerned with the issue of char-N partition between NO and N_2O and are not discussed in this paper since at pulverized combustion conditions NO is the main pollutant.[4] Few models are specifically targeted to the pulverized combustion regime. The approach of the pioneering work of Wendt and Schulze[5] has been followed by different authors.[6,7] In Visona and Stanmore's model[6] char-N may evolve as NO, HCN and N_2. These authors tested different rates for NO reduction on the char, as well as the effect of CO concentration. They concluded that most of the expressions reported in the literature for the reduction of NO on char surface were too low to predict the amount of char-N converted to NO. Jensen et al[7] found in a fixed bed reactor that large sample size produced a low conversion of char N to NO as a result of NO reduction on the char surface when *in situ* generated chars were oxidized under $10\%O_2/N_2$. They also suggested that most of the rates for the NO-char reaction reported in the literature for oxygen-free conditions were too low to explain the evolution of char-N to NO and proposed the necessity for the evaluation of the NO-char reaction when oxygen is present.

These two studies cast doubt on the convenience of the use of most of the kinetic expressions for the rate of NO reduction on the surface when predicting char-N evolution to NO. This reaction seems therefore to be a critical element in modeling NO production during char combustion. Since it is not the main objective of this paper to discuss this reaction, the reader is referred to different reviews on this topic.[8-10] Nevertheless it may be helpful for further discussion to draw attention to two points. First the effect of CO through the reaction:

$$CO + NO \xrightarrow{char,k_{NO-CO}} 0.5N_2 + CO_2 \qquad \text{R 1}$$

R 1 occurs in parallel to the global NO-char reaction:

$$NO + C \xrightarrow{k_{NO}} 0.5N_2 + CO \qquad \text{R 2}$$

Secondly in the effect of O_2, Chambrion et al[11] found that O_2 has a catalytic effect on R 2. The fact that their experiments were at 600°C and low O_2 concentration (0.4%) makes the comparison of the results to the PC conditions difficult. No analytical expression was found in the reviewed literature for the quantification of the effect of O_2 on this reaction.

This study proposes a single particle model that predicts the formation of NO from char-N. This model is compared to the experimental data obtained in a drop tube reactor, at temperatures similar to those of pulverized bed combustors. The rate of NO reduction on char was also evaluated in order to be used as an input for the model.

REACTOR AND EXPERIMENTAL SETUP

The experiments were carried out in an electrical heated laminar flow drop tube reactor with a cross sectional diameter of 5.08×10^{-2} m. The conventional setup of the drop-tube was modified to allow the implementation of batch experiments and *in situ* char formation.

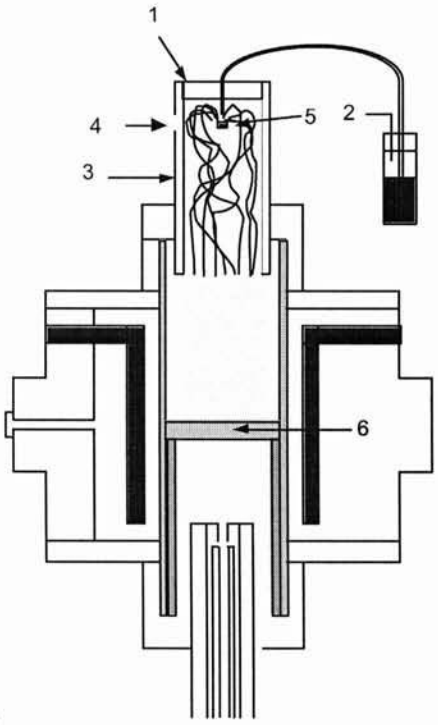

Figure 1. Experimental setup for the Batch experiment. **1.** Quartz window. **2.** Carrying gas input. **3.** Distributor. **4.** Distributor radial gas. **5.** Bluff disk. **6.** Alumina/silica no woven fabric

Figure 1 presents a schematic of the experimental setup. During the experiments, a known amount of coal or char was introduced to the reactor under inert or oxidizing atmosphere by means of a custom-built distributor part. This distributor part is composed of a disk located in front of the char injection tube. The purpose of the disk is to generate a turbulent zone that spreads the coal uniformly over the entire cross-sectional area of the drop tube reactor, minimizing the chance of particle-particle interactions. To prevent the deposition of coal on the walls of the distributor, a radial gas stream is injected through the walls of the distributor surrounding the coal injection zone. After the disk, laminar flow develops before the gases enter the drop tube reaction zone and the coal stream is dispersed over the entire cross sectional area. Since the flow inside the reacting section is laminar, no deposition of coal on the reactor walls occurs. The solid stream is then collected over an alumina/silica non-woven fabric that was placed in the medium of the reacting zone. A quartz window on the top of the drop tube allowed visual examination of the particle distribution. The exhaust gases are collected by a water-cooled probe placed immediately under the non-woven fabric. Analysis of CO, CO_2, NO, NO_2, N_2O and HCN was performed by FTIR. For some experiments, CO, CO_2 FTIR concentrations were verified with a NDIR analyzer, as well as NO concentration by a chemiluminescent analyzer.

Three different experiments were conducted:

1. **Oxygen-free experiments**. The objective of this set of experiments was to evaluate the rate of NO reduction on char surface. In this case coal or char was injected into an NO/He stream and then collected on the non-woven fabric. The reduction rate of NO reduction by the char was computed as follows:

$$k_{NO} = \ln\left(\frac{C_{NO}^{in}}{C_{NO}^{out}}\right)\frac{v}{w_{char}} \qquad \text{E 1}$$

E 1 assumes a first order reaction between NO and char. After five minutes, O_2 is injected in the reactor and the value of w_{char} is obtained from the integral of the concentrations of carbon oxides detected in the product gases.

2. ***In situ* char experiments.** For these experiments, coal was introduced to the reactor under inert atmosphere. After 60s under inert atmosphere, an O_2-containing stream is introduced to the drop tube and the chars are rapidly consumed during oxidation. The purpose of this experiment was to evaluate the conversion of char-N to NO for chars prepared *in situ*. However, NO reduction in the downstream section of the reactor due to the fuel-rich conditions in the combustion gas after char oxidation complicated the interpretation of this set of experiments.

3. Direct injection. To avoid any reduction of the NO produced during reaction, char or coal was injected into an O_2-containing stream. In this way char oxidation begins while the particle is falling in the reactor. The residence time for the particle in suspension is less than 300 ms; since this is less than the time for oxidation, the reaction is completed in the non-woven fabric. The sample size for all experiments was ~ 5 mg. The total gaseous flow was 4000 sccm.

COAL AND CHAR SAMPLES

In order to understand the effect of the carbonaceous material on reaction R 2 as well as on the amount of char-N that is converted to NO, an Illinois No. 6 coal and two different chars were used in the experiments. An activated char with low nitrogen content was included for comparison. Table 1 presents the ultimate and proximate analysis of the samples. Coal refers to the raw Illinois No. 6 coal. Char DT refers to char produced by injection of coal in a **D**rop **T**ube reactor without the presence of the non-woven fabric (continuous injection mode); the char from the drop tube provides the elemental and proximate analysis for the initial condition of the char in the *in situ* experiment explained above. Char U-Furnace is char produced in a pulverized coal pilot scale furnace[12] from Illinois No.6 coal under a self-sustained flame and under typical pulverized combustor conditions. And finally, activated char is the commercial activated char produced from coconut shell.

Table 1. Coal and Char analysis

	Proximate Analysis				Ultimate Analysis (daf)				
	Moist.	Ash	Volatile Matter	Fixed Carbon	C	H	N	S	O
Coal	6.91	5.56	46.38	41.15	80.67	5.30	1.87	0.98	11.19
Char DT	5.30	10.86	4.07	85.07	95.70	0.56	1.84	0.72	1.18
Char U-Furn.	0.89	17.85	N.A.	N.A.	92.63	1.48	1.96	0.62	3.31
Activat. char	6.06	5.23	N.A.	N.A.	91.56	2.06	0.14	0.02	6.21

N.A. Not available

SINGLE PARTICLE MODEL

The single particle model developed in this study solves the species conservation equation (E 2) for all the gaseous species involved in the system (CO, N_2, NO, O_2 and He) and for one solid species, carbon in the char. It assumes the system to be isothermal. The particle temperature was assumed to be 100 K higher than the gas temperature as suggested from the experimental results of Hurt[13] for Illinois No. 6 char.

$$\frac{\partial}{\partial t} c_i = -\left(\frac{1}{r^2} \frac{\partial}{\partial r} \left(r^2 N_i \right) \right) + R_i^v \qquad \text{E 2}$$

E 2 was solved by applying a control volume technique as described by Patankar.[14] The molar flux, N_i is assumed to be in the Knudsen regime, therefore it is approximated to be a diffusion flux, as given by E 3

$$J_i = -D_{k,i} \frac{dC_i}{dr} \qquad \text{E 3}$$

The coefficient of Knudsen diffusivity is the one recommended by Satterfield[15] (E 4) and was computed for every species. The tortuosity was assumed to by 2.

$$D_{K,i} = \frac{8}{3} \left(\frac{\theta}{A_s \rho_p} \right) \sqrt{\frac{2R_g T}{\pi MW_i}} \qquad \text{E 4}$$

For the carbon oxidation, the intrinsic reaction rate of Smith[16] was used.

$$R_i = 3050 \exp(-179.4/RT) \quad \frac{kgC}{m^2 s (101325 PaO_2)}, \text{ original expression} \qquad \text{E 5}$$

$$R_i^C = 2.5061 \exp(-2.1578 x 10^4 / T) \quad \frac{gmolC}{m^2 s PaO_2}, \text{ Expression for } R_i \qquad \text{E 6}$$

$$R_C^v = R_i^C * C_{O_2} * R_g * T * A_{s\_v} \quad \frac{gmolC}{m^3 s} \qquad \text{E 7}$$

Where

$$A_{s\_v} = C_C * MW_C * \frac{1}{C\_\%} * A_s * \frac{1}{1000} \quad \frac{m^2}{m^3} \qquad \text{E 8}$$

The char surface area (A_S) was considered to change with char conversion as defined by[17]:

$$A_s = A_s^o (1 + 2.5X)(1 - X) \qquad \text{E 9}$$

An initial particle surface area of 100 m²/gm for the coal chars and of 1400 m²/gm for the activated char was used for all the models.

The rate of NO production was assumed to be proportional to the rate of C_S consumption. With N/C, (atomic ratio of N to C in the char at 0 burnout) as proportionality constant.

$$R_{NO}^v = R_C^v * N/C \quad \frac{gmolNO}{m^3 s} \qquad \text{E 10}$$

The volumetric void pore fraction of the particle, or char porosity is taken from Stanmore[17] as:

$$\theta = \theta_o + X(1 - \theta_o)\theta_c \qquad \text{E 11}$$

With θ_o as 0.41.

The boundary conditions were symmetry at $r = 0$ and at $r = R_p$ the a flux is given by the following expression:

$$N_{i,r=R_{nr}} = -k_g (c_i^{bulk} - c_i^{nr}) \qquad \text{E 12}$$

k_g, the mass transfer coefficient was computed as:[18]

$$k_g = D_{eff} / (2 * R_p) \qquad \text{E 13}$$

D_{eff}: Mass transfer effective multicomponent effective diffusion coefficient, computed by CHEMKIN II transport package.[19]

RESULTS AND DISCUSSION

1. Oxygen-free experiments

Since several of the values present in the literature for the rate of NO reduction on char surface (e.g.[20-23]) have been considered too low to account for the conversion of char-N to NO by recent studies,[6,7] experiments to establish the value of k_{NO} for the present set-up and chars were carried out.

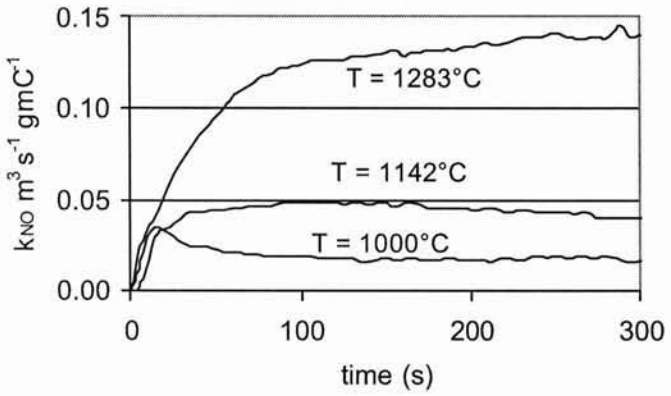

Figure 2. Rate of NO reaction on char produced from Illinois No.6 coal. Coal was injected on the top of the reactor to a 740ppm NO/He stream at time 0.

Figure 2 presents the rate of NO reduction as computed from E 1 for Illinois No.6 chars. In this experiment, coal was injected at time 0 and the rate was computed from this initial time. The first result to point out from Figure 2 is from the plot at 1000°C. At this temperature, and at the initial time there is a small increase in the reaction rate. These results are similar to those of Jensen et al.[7]

However, at higher temperatures this effect is not observed. Figure 3 presents the molar ratio of NO/C (C refers to the sum of the carbonaceous species, mainly CO, in the product gases) and HCN/C for the experiment at 1000°C in Figure 2. The results suggest a high HCN production during the first initial period of the reaction, when pyrolysis is occurring. After the pyrolysis reactions decay the NO/C ratio increases to one, as is expected from R 2, and the HCN/C ratio drops to a very low value. Plots similar to Figure 3 were prepared at other temperatures and the values of HCN/C were considerable lower for the other two cases. This information suggests that the evaluation of k_{NO} at times prior to completion of pyrolysis may be biased by the reactions of NO with pyrolysis products. Given the nature of the expression for the evaluation of k_{NO} (E 1), the value of the w_{char} is critical for the final results of k_{NO}. If the mass of char is underestimated by

neglecting the production of carbon-containing species (such as HCN) the value of k_{NO} increases, in the case of Figure 2 by 30%. This effect may be less pronounced at higher temperatures since the times for late devolatilization reactions will be lower. The value k_{NO} was computed when a plateau in the value of k_{NO} was obtained for all the temperatures in order to eliminate the transient initial reaction with the pyrolysis products. Table 2 presents the results of Arrhenius plots obtained from data similar to Figure 2 for other materials.

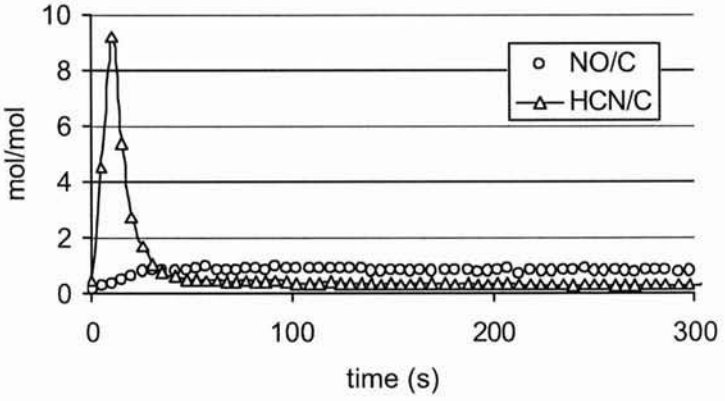

Figure 3. NO/C and HCN/C ratios for the NO-char reaction. Coal Illinois No. 6. T = 1000°C

Table 2. Values for the reaction of char with NO for different chars

	ko (m^3/s gm C)	Ea (J/gmol K)	r
Char U furnace	26439	152306	0.9972
Coal Illinois No. 6	1323	118589	0.9947
Activated char	27515	148748	0.9995

Figure 4 presents the comparison of the kinetic expressions of Table 2 to those of the general expression derived by Aarna and Suuberg.[8]. The char-NO kinetics differ by less than one order of magnitude. Most of the results are in the upper range of the generalized expression given by E 14. Furthermore, there is not a great difference between the values reported for NO reduction on char for *in situ* chars and the one prepared *a priori*.

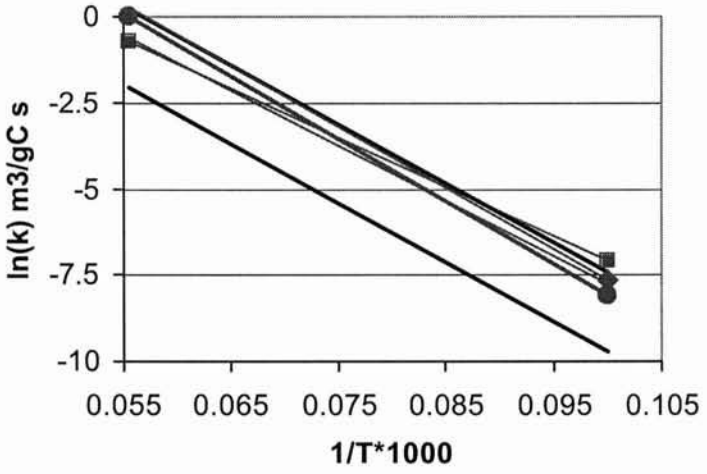

Figure 4. Arrhenius plots for the reaction NO-char for four different solids. Bold lines represent general expression by Aarna and Suuberg[8] and one order of magnitude this value. Squares: Coal; Circles: Char U furnace; Diamonds: Activated char

$$k_{NO} = 5.5\times10^{6}\exp(-15939/T)\ \mathrm{g_{NO}m^{-2}h^{-1}\ atm_{NO}^{-1}} \qquad \text{E 14}$$

2. Experiments in the presence of oxygen

As discussed before, the rate of NO reduction on char surface seems to have a strong influence on the prediction of single particle models on the amount of char-N converted to NO. The conversion of char-N to NO for different bulk-NO concentrations was evaluated to check previous findings that the rate of NO reduction in oxygen free environment was first order with respect to NO, particularly in the high temperature regime.[24]

In order to do this, the variable α_{NO}, as defined by E 15, was chosen to represent the amount of char-N converted to NO. Note that α_{NO} can be negative in case the reaction of the NO injected as background gas is greater than the NO formed from char nitrogen oxidation.

$$\alpha_{NO} = \frac{\int_{t_1}^{t_2} v(C_{NO}^{out} - C_{NO}^{in})dt}{(N/C)_{solid}\int_{t_1}^{t_2} v(C_{CO}^{out} + C_{CO2}^{out})dt} \qquad \text{E 15}$$

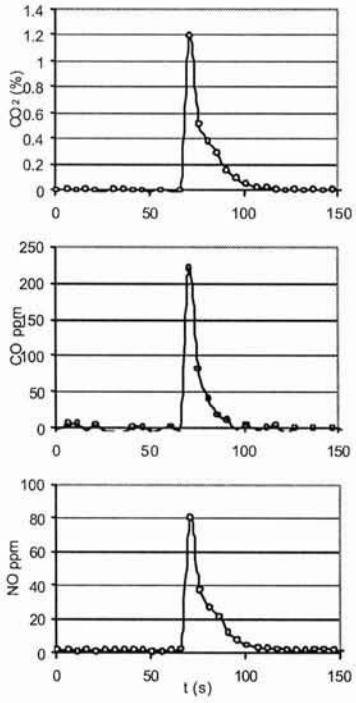

Figure 5. Combustion gases concentration during char U-furnace oxidation. *Tg*=1698K. 4%O2/He. *Dp*= 58μm.

Figure 5 presents the concentration of combustion products from the combustion of char U-Furnace when NO background was zero. Similar results were obtained from the other solid samples.

Although the duration of the char oxidation reaction is in the order of 1 second, the residence time in the analysis trail accounts for the broad peak in Figure 5. It is clear that the FTIR doesn't allow resolving the concentrations in time. However, the data are sufficient for the calculation of α_{NO} and the carbon balance was between 85% and 110% for all the experiments. No specific trend in carbon balance was observed as the NO concentration was increased.

Figure 6 presents the results of α_{NO} for three different solids: chars U-furnace, coal and activated char. The first striking result is that the plot of α_{NO} vs. NO concentration in the background lied in straight lines for all three solids. An almost linear relation was also obtained by Spinti[25] in similar experiments performed in a pilot-scale pulverized coal boiler.[12] This result, although surprising, may be explained in a rather simple way by considering the effect of the rate of NO reduction on the char surface. α_{NO} can be also defined by:

$$\alpha_{NO} = \frac{NO^{out} - NO^{in}}{NO_{solid}^{tot}} \qquad \text{E 16}$$

Where NO_{solid}^{tot} represents the amount of NO produced from the solid if all the nitrogen in the solid were converted to NO, and NO^{out} and NO^{in} represent the integrated amounts of NO leaving and entering the reactor, respectively. Note that $NO^{in} = NO^{bkg} + NO^{solid}$,

where NO^{bkg} represents the NO injected in the background and NO^{solid} the one produced by the solid. Since for these experiments, a rather small sample was used compared to the total gas flow, $NO^{bkg} >> NO^{solid}$, therefore $NO^{in} \sim NO^{bkg}$. From E 1 and E 16 it follows that:

$$\alpha_{NO} = \frac{NO^{bkg}\left(\exp\left(\frac{-k_{NO} w_{char}}{v}\right) - 1\right)}{NO^{tot}_{solid}} \qquad \text{E 17}$$

E 17 presents a linear relation between α_{NO} and NO^{bkg} and explains why the plot is so similar for the coal Illinois No. 6 and the char U-furnace. In the previous section, k_{NO} was found to be similar for the char prepared *in situ* from Illinois No. 6 coal and for the char U-furnace. If this is the case, for a given NO^{in}, α_{NO} will only differ from the two solids in the value of NO^{tot}_{solid}. Given similar sample weights and since the nitrogen content of both solid is comparable (Table 1), α_{NO} will be similar for both samples. E 17 also predicts, in accordance to the results in Figure 6, that the activated carbon, with a lower value of NO^{tot}_{solid}, will present a higher slope for the plot of α_{NO} vs. NO^{bkg}.

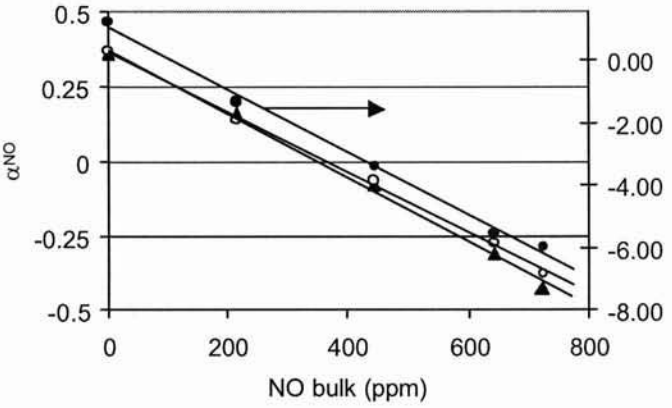

Figure 6. Variation of the conversion of solid-N to NO during oxidation expe riments. T_g = 1698 K. 4%O_2. D_p = 58μm. ○: Char U-Furnace(left axis); ? :Coal Illinois No. 6 (left axis); ●:Activated char (right axis)

Although expression E 17 gives explanation to many of the experimental facts observed during the combustion of the carbonaceous materials used in this study, it may not be easily applied to a the combustion of a char particle, since it was designed for a steady-state system. Nevertheless, the important information obtained from E 17 is that any single particle model for the prediction of char-N evolution to NO should consider a first order reaction of NO with char.

3. Single particle model and prediction of char-N evolution

As a final part in the analysis, the single particle model described before was applied to the combustion of char with NO as background gas. From the prior discussion, it is clear that the rate of NO reduction on the char surface is a very important parameter in the model. Therefore, as a first approach, the values of k_{NO} determined in the oxygen-free experiments were used as inputs for the model and only reaction R 2 was considered for the destruction of NO on char surface. The open symbols in Figure 7 represents the results of this comparison. Although the model predicts the reduction of α_{NO} when the NO bulk concentration increased in a lineal way , the estimated values for α_{NO} are higher

than the values found experimentally. Similar results were obtained for the other chars. To better understand the model predictions, Figure 8 presents the variation of the species concentration during char oxidation when char conversion was 0.4. C_s represents the ratio of carbon concentration at time t to that at the beginning of the reaction. According to the model predictions, the reaction of carbon oxidation occurs in a narrow range in the external part of the particle. This results justifies the traditional practice of computing the rate of carbon-oxygen reaction on an external surface area basis.[26]

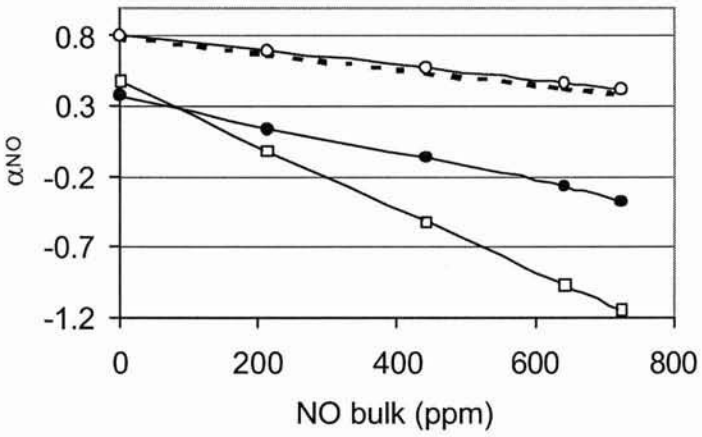

Figure 7. Comparison of model prediction with experimental data for the oxidation of char U-furnace T_p = 1800 K. D_p = 58μm. 4.0%O_2/640 ppm NO/29.4%N_2/66%He ●: Experimental data ○Model (Only R 2); Dotted line: Model (R 2 and R 1) □: Model (R 2 and R 1) and k_{NO}*10

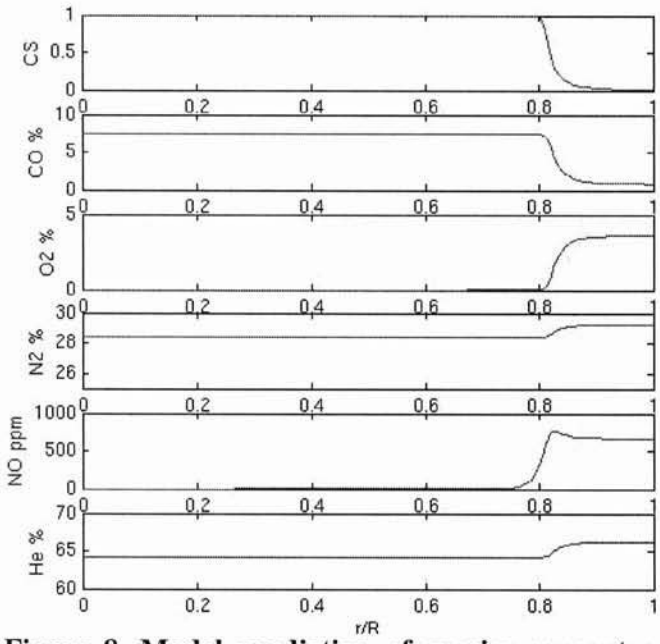

Figure 8. Model prediction of species concentration vs. non-dimensional particle radius for the oxidation of char U-furnace T_p = 1800 K. D_p = 58μm. 4.0%O_2/640 ppm NO/29.4%N_2/66%He Char conversion was 0.40.

NO is produced in the same narrow region of carbon oxidation, and it can diffuse inside the particle, where it is rapidly reduced on the char, or escape to the boundary layer. Due to the fast reaction of carbon with oxygen, the carbon concentration in this region is low, and a considerable amount of NO escapes to the boundary layer without been reduced by the particle. Figure 8 also shows that in the same region, the CO concentration is high, as it is expected from the char oxidation. Under this conditions, reaction R 1 may be important in the process of NO destruction. Therefore, the kinetics of NO destruction, by CO on char surface was incorporated to the model. For R 1, Aarna and Suuberg[27] found that the

reaction was zero order with respect to CO, particularly for high CO concentrations, and first order with respect to NO at high temperatures. They also suggested expression E 18 as a possible value for reaction R 2.

$$k_{NO-CO} = 1.2 \times 10^{6} \exp(-13919/T)\ g_{NO} m^{-2} h^{-1} atm_{NO}^{-1} \qquad \text{E 18}$$

Expression E 18 was incorporated to the model, but there was not significant improvement in model predictions (see Figure 7). Finally, for comparison, the effect of an increase in one order of magnitude in k_{NO} was evaluated. The results in Figure 7 show that although there is a reduction on the value of α_{NO} at low NO bulk concentration, the slope of the plot differs from the one found in the experiments. This suggests, that the reason for the disagreement between model predictions and experimental results may not be only related to the value of k_{NO}, but also to another factor, possible a larger area of char in contact with NO than the one predicted using a single particle size and Knudsen diffusivity.

CONCLUSIONS

It is important to guarantee that the pyrolysis reactions have decayed during the determination of the rate of NO reduction on char surface. Otherwise, unrealistic high values of k_{NO} will result due to underestimation of the char sample and due to reactions between NO and the pyrolysis byproducts.

The rates of NO reduction on char for the carbonaceous materials used in this study were similar. These results, coupled to the first order reaction of NO on the char surface explain why plots for the conversion of char-N to NO vs. NO bulk concentration are linear and are almost independent on the nature of the carbon material used. These results, underscore the importance of the reaction of char with NO since suggest that char particles surrounded by low NO concentrations, as those expected in new low-NO burners, will produce more NO from char-N, than particles exposed to higher NO concentrations. The similarity of the curves of conversion of char-N to NO vs. NO concentration (Figure 7) suggests that under the experimental conditions of this study, the heterogeneous reactions dominate the reduction of the NO that evolves during char oxidation.

A single particle model for the evolution of char-N to NO was developed. The model correctly predicts the linear decrease of char-N conversion to NO as the NO bulk concentration is increased. However, the model overpredicts NO production. The reason for this is unclear, but seems to be related to the availability of char surface for NO reaction during char combustion predicted using a simplistic single pore size diffusion model. Future modeling will explore the impact of multimodal pore diffusion models.

NOMENCLATURE

A_s: Surface area of the particle (kg m^{-2})
A_{s_v}: Internal surface area of the char per reactor volume (m^2 m^{-3})
C_i^{in}: Concentration of species i at reactor's entrance (mol/m^3)
C_i^{out} Concentration of species i at reactor's exit (mol/m^3)
c_i: Molar concentration of species i (gmol m^{-3})
D_{eff}: Mass transfer effective multicomponent diffusion coefficient (m s^{-2})
D_p: Particle average diameter (m)
$D_{k,i}$ Knudsen diffusivity of species i
J_i: Molar diffusive flux if species i (mol m^{-2} s^{-1})
k_g: Mass transfer coefficient (m s^{-1})
k_{NO} Rate of NO-char reaction (m^3/gmC s)
$(N/C)_{solid}$ Nitrogen to carbon molar ratio in the injected solid (-)
N_i: Molar flux of species i (gmol m^{-2} s^{-1})
R_i^v: Volumetric molar rate of formation of species i (gmol m^{-3} s^{-1})
R_i^C: Intrinsic rate for the reaction carbon oxygen
v: Volumetric flow (m^3/seg)
w_{coal}: Weight of sample in the reactor (gm of C)
T_g: Gas temperature (K)
r: Particle radius at time t (m)

θ: Char porosity (-)
θ_o: Char porosity at beginning of reaction (-)
θ_c: Ratio char solid volume to char total volume (-)

$$\theta_c = 1 - f_{ash}\frac{\rho_p}{\rho_{ash}}$$

f_{ash}: Initial ash mass fraction of the char
ρ_{ash}: Ash density (kg m^{-3})
ρ_p: Particle density (kg m^{-3})

REFERENCES

1 de Soete, G. G., Croiset, E. and Richard, J.R. Combustion and Flame 1999, 117, 140
2 Winter, F., Warth, C., Loffler, G. and Hofbauer, H. Twenty-sixth Symposium (International) on Combustion/ The Combustion Institute 1996, 3325
3 Goel, S., Morihara, A., Tullin, C. and Sarofim, A. Twenty-Fifth Symposium (Int.) on Combustion/The combustion Institute 1994, 1051
4 Pershing, D.W. and Wendt, J. Sixteenth Symposium (International) on Combustion/ The Combustion Institute 1976, 389
5 Wendt, J. and Schulze, O. AIChE Journal 1976, 22, 102
6 Visona, S. and Stanmore, B. Combustion and Flame 1996, 106, 207
7 Jensen, L.S., Jannerup, H.E., Glarborg, P., Jensen, A. and Dam-Johansen, K. Twenty-eight Symposium (International) on Combustion/ The Combustion Institute 2000
8 Aarna, I. and Suuberg, E. Fuel 1997, 76, 475
9 Li, Y.H., Lu, G.Q. and Rudolp, V. Chemical Engineering Science 1998, 53, 1
10 Molina, A., Eddings, E.G., Pershing, D.W. and Sarofim, A.F. Prog. Energy Combust. Sci. 2000, 26, 507
11 Chambrion, P., Kyotani, T. and Tomita, A. Twenty-seventh Symposium (International) on Combustion/ The Combustion Institute 1998, 3053
12 Spinti, J.P., Pershing, D. W., Brouwer, J. and Heap, M.P. Combustion Science and Technology 1997, 126, 1
13 Hurt, R. Energy & Fuels 1993, 7, 721
14 Patankar, S.V. Numerical Heat Transfer and Fluid Flow, 1980, Taylor and Francis Ed
15 Satterfield, C.N. Heterogeneous Catalysis in Industrial Practice, 2nd Ed. 1991, McGraw-Hill, Inc
16 Smith, I. Fuel 1978, 57, 409
17 Stanmore B.R. Combustion and Flame 1991, 83, 221
18 Smith, I.W. Nineteenth Symposium (International) on Combustion/ The Combustion Institute 1982, 1045
19Kee, R.J., Dixon-Lewis, G., Warnatz, J., Coltrim, M.E., Miller, J.A. Sand86-8246, 1986
20 Chan, L., Sarofim, A. and Béer, J. Combustion and Flame 1983, 52, 37
21 Song, Y., Beér, J. and Sarofim, A. Combustion Science and Technology 1981, 25, 237
22 de Soete, G. Twenty-Third Symposium (International) on Combustion/The Combustion Institute 1990, 1257
23 Levy, J., Chan, A., Sarofim, A., and Beér, J. Eighteenth Symposium (International) on Combustion/The Combustion Institute 1981, 111
24 Aarna, I. and Suuberg, E. Twenty-seventh Symposium (International) on Combustion/ The Combustion Institute 1998, 3061
25 Spinti, J. Ph.D. Thesis, University of Utah 1997
26 Hurt, R.H. and Mithcell, R.E. Twenty-Fourth Symposium (Int.) on Combustion/The combustion Institute 1992, 1243
27 Aarna, I, and Suuberg, E.M. Energy & Fuels 1999, 13, 1145